Jchain-driven cre enables specific genetic manipulation and timestamping of plasma cell in their niche.

Xu AQ[1], Barbosa RR[1], Calado DP[1,2,3*]

1. Immunity and Cancer, The Francis Crick Institute, 1 Midland Road, London NW1 1AT, UK.
2. Peter Gorer Department of Immunobiology, School of Immunology & Microbial Sciences, King's College London, London, UK.
3. Lead contact.

* Corresponding author: Dinis.Calado@crick.ac.uk

Keywords

Jchain, *Blimp1*, *Irf4*, plasma cells, B cells, cre-loxP

Highlights

- *Jchain*-driven cre-mediated genetic manipulation is effective only in plasma cells
- *Jchain* expression occurs in plasma cells across immunoglobulin isotypes
- Genetic manipulation using Jchain-driven cre targets plasma cells already in their niche
- *Jchain*-driven cre allows tracing of long-lived plasma cells

Summary

Plasma cells are essential for long-term protection from infection and underlie vaccination success. However, studies of gene function in plasma cells are hindered by technical limitations. Here we report an engineered allele that allows to trace and genetically manipulate plasma cells.

Abstract

Plasma cells produce antibodies that are essential for protection from infection and for vaccination success. Plasma cells are also at the origin of currently incurable hematological malignancies, most notably multiple myeloma. However, the study of gene function in plasma cells has mostly been performed using *in vitro* cultures and cell transfer systems that remove plasma cells from their microenvironment. Further, existing systems to genetically manipulate plasma cells are not specific and target multiple cell lineages including B cells, making it difficult to discriminate gene function in plasma cell formation and/or maintenance. Here we characterized a genetically engineered allele: *Igjcre*$^{ERT2(GFP)}$ that expresses GFP and cre^{ERT2} under the activity of the endogenous *Jchain* promoter. We found at the single cell level that *Jchain* expression occurred in plasma cells across immunoglobulin isotypes. Also using the *Igjcre*$^{ERT2(GFP)}$ we performed highly specific cre-loxP genetic manipulation of plasma cells residing in their natural microenvironment *in vivo* in the mouse and traced long-lived plasma cells.

57 **Introduction**

58 Plasma cells produce antibodies that are crucial for immune protection against infection and for
59 vaccination success (Nutt et al., 2015). Upon activation, B cells terminally differentiate into plasma
60 cells, a process initiated by the downregulation of the B cell transcription factor PAX5 (Kallies et al.,
61 2007). This event allows the expression of multiple factors normally repressed by PAX5, including
62 *Xbp1*and *Jchain* (Castro and Flajnik, 2014; Nutt et al., 2015; Rinkenberger et al., 1996; Shaffer et al.,
63 2004). PAX5 downregulation is also followed by the expression of the transcription factors IRF4 and
64 BLIMP1 that are essential for the establishment of the plasma cell program (Kallies et al., 2007; Klein
65 et al., 2006; Shapiro-Shelef et al., 2003). Beyond physiology, multiple cancers have a plasma cell as
66 the cell of origin, including multiple myeloma that is the second most frequent hematological
67 malignancy overall and for which a cure remains to be found (Palumbo and Anderson, 2011). As
68 consequence, the study of gene function in plasma cell homeostasis is a subject of intense investigation.
69 However, because of the lack of tools many studies make use of *in vitro* and cell transfer systems that
70 remove plasma cells from their microenvironment. Further, genetic manipulation of plasma cells is
71 currently not specific, targeting other cellular populations including B cells. These strategies are limited
72 in their ability to study gene function in plasma cells in their microenvironment and confound plasma
73 cell formation and maintenance.

74 We found that amongst plasma cell associated genes, *Jchain* (*Igj*) had the highest level and most specific
75 expression in plasma cell populations. JCHAIN is a small polypeptide that is required to multimerize
76 IgM and IgA and that is necessary for the transport of these Ig classes across the mucosal epithelium in
77 a poly-Ig receptor mediated process (Brandtzaeg and Prydz, 1984; Castro and Flajnik, 2014; Max and
78 Korsmeyer, 1985). Here, we characterized a GFP-tagged cre^{ERT2} allele: *Igjcre$^{ERT2(GFP)}$* at the *Jchain*
79 endogenous locus. At the single cell level *Jchain* expression occurred in plasma cells across
80 immunoglobulin isotypes, including IgG1. Using the *Igjcre$^{ERT2(GFP)}$* we performed highly specific cre-
81 loxP genetic manipulation of plasma cells residing in their natural microenvironment *in vivo* and traced
82 long-lived plasma cells. *Igjcre$^{ERT2(GFP)}$* is a validated allele for plasma cell studies, allowing the
83 mechanistic understanding of gene function in plasma cells *in vivo* and in their niche.

84

85 **Results**

86 ***Jchain* transcripts are highly enriched in plasma cell populations**

87 B-to-plasma cell differentiation is a process that involves a complex network of factors (**Fig. 1A**; (Nutt
88 et al., 2015)). We investigated the level and specificity of the expression of genes associated with
89 plasma cells (*Xbp1*, *Jchain*, *Scd1*, *Irf4*, and *Prdm1*) through the analysis of a publicly available RNA
90 sequencing dataset (ImmGen, (Heng et al., 2008)). We first determined the cell populations with the
91 highest transcript level for each factor (**Fig. 1B**). *Xbp1* and *Irf4* were primarily expressed in plasma cell
92 populations, however the expression in bone marrow plasma cells (B_PC_BM) was less than 2-fold
93 greater than that of non-plasma cell populations (**Fig. 1B**). The expression of *Sdc1* and *Prdm1* was not
94 specific to plasma cell populations (**Fig. 1C**). Peritoneal cavity macrophages (MF_226+II+480lo_PC)
95 expressed more *Sdc1* than bone marrow plasma cells (B_PC_BM), and a subset of FOXP3^{+} cells
96 (Treg_4_FP3+_Nrplo_Co) expressed higher levels of *Prdm1* than that observed in splenic plasmablasts
97 (B_PB_Sp) and bone marrow plasma cells (B_PC_BM; **Fig. 1C**). In contrast, *Jchain* had the highest
98 level of transcript expression in plasma cell populations compared to non-plasma cells and was the most
99 plasma cell specific amongst all factors, with a 40-fold enrichment over germinal center (GC) B cells
100 (B_GC_CB_Sp; **Fig. 1D**). We concluded that the *Jchain* was a suitable candidate for genetic
101 engineering and generation of plasma cell specific tools.

102

103 ***Jchain* is expressed in a small fraction of GC B cells and in most plasma cells**

104 We searched alleles produced by the EUCOMMTools consortium and identified a genetically
105 engineered *Jchain* allele produced by the Wellcome Trust Sanger Institute: MGI:5633773, hereafter
106 termed: *Igjcre$^{ERT2(GFP)}$*. The genetically engineered *Jchain* allele contained an *FRT* site between exons
107 1 and 2 followed by an engrailed 2 splice acceptor sequence and an *EGFP.2A.cre^{ERT2}* expression
108 cassette (**Fig. 2A**). In this design the expression of the EGFP (GFP) and of cre^{ERT2} is linked by a self-
109 cleaving 2A peptide under the transcriptional control of the *Jchain* promoter (**Fig. 2A**). To determine
110 cells with GFP expression we initially analyzed the spleen from mice heterozygous for the *Igjcre$^{ERT2(GFP)}$*
111 allele that had been immunized 12 days earlier **(Fig. 2B)**. B220 is expressed on the surface of B cells
112 and downregulated during plasma cell differentiation (Pracht et al., 2017). We therefore defined three

113 cell populations based on the levels of GFP fluorescence and B220 surface expression: $GFP^{low}B220^{high}$,
114 $GFP^{int}B220^{int}$, $GFP^{high}B220^{low}$, and a population negative for both markers ($GFP^{neg}B220^{neg}$; **Fig. 2C**).
115 We next determined the fraction of cells within these populations expressing surface CD138, that is a
116 commonly used marker to define plasma cells by flow-cytometry (Pracht et al., 2017). The
117 $GFP^{neg}B220^{neg}$ population did not contain $CD138^{+}$ cells, however, the fraction of $CD138^{+}$ cells
118 increased in the remaining populations in agreement with the reduction of B220 during plasma cell
119 differentiation, with the $GFP^{int}B220^{int}$ and $GFP^{high}B220^{low}$ populations being mostly composed of
120 $CD138^{+}$ cells (**Fig. 2D** and **E**). Identical results were observed when defining plasma cells using an
121 additional marker, the CXCR4 chemokine receptor that facilitates homing of plasma cells to the bone
122 marrow (**Fig. 2D** and **E**; (Hargreaves et al., 2001)). We investigated the cellular composition of the
123 $GFP^{low}B220^{high}$, that contained the fewest $CD138^{+}$ cells (1 to 20%; **Fig. 2E**). We found that virtually all
124 $CD138^{neg}$ cells within $GFP^{low}B220^{high}$ expressed the B cell marker CD19 (**Fig. 2F**). Also and in
125 agreement with *Jchain* gene expression analysis (**Fig. 1D**) these cells were mostly GC B cells
126 ($CD38^{low}FAS^{high}$; **Fig. 2F** and **G**). We also performed analyses in the spleen and bone marrow of 12-
127 day immunized mice heterozygous for the $Igjcre^{ERT2(GFP)}$ allele in which mature and B cell precursors
128 as well as non-B cell populations were first defined using surface markers and the fraction of GFP
129 expressing cells within those populations determined (**Fig. S1**). We found that a small fraction of B1b
130 cells (0 to 6%) in the spleen and most plasma cells ($CD138^{+}CXCR4^{+}$, 60 to 90%) in the spleen and
131 bone marrow expressed GFP (**Fig. S1**). B1b cells are prone to differentiate into plasma cells and are a
132 source of IgM antibodies upon T cell independent responses (Alugupalli et al., 2004). Collectively these
133 data confirmed at the single cell level the analysis of gene expression using bulk populations (**Fig. 1D**)
134 and suggested that *Jchain* expression is enriched in plasma cells.
135

136 ***Jchain* expression correlates with IRF4 and BLIMP1 co-expression**

137 IRF4 and BLIMP1 transcription factors play an essential role in plasma cell differentiation (Kallies et
138 al., 2007; Klein et al., 2006; Shapiro-Shelef et al., 2003). We therefore analyzed the spleen of 12-day
139 immunized mice heterozygous for the $Igjcre^{ERT2(GFP)}$ allele and determined whether IRF4 and BLIMP1
140 were expressed in the populations defined by varied GFP and B220 surface expression (**Fig. 2C**, **3A**

141 and **B**). The GFP^{neg}B220^{neg} cells were virtually devoid of BLIMP1 and IRF4 expression (**Fig. 3C**). In
142 contrast the GFP^{low}B220^{high} cell population contained ~7% (median) of BLIMP1^{+}IRF4^{+} cells (**Fig. 3D**
143 and **E**). This suggested that *Jchain* expression can precede that of IRF4 and BLIMP1, something
144 previous suggested from *in vitro* cultures of *Blimp1* deficient B cells (Kallies et al., 2007). Still,
145 increased *Jchain* expression strongly correlated with that of IRF4 and BLIMP1 as the vast majority of
146 cells within the GFP^{int}B220^{int} and GFP^{high}B220^{low} populations were BLIMP1^{+}IRF4^{+} (**Fig. 3D** and **E**).
147 These data confirmed *in vivo* the observations of others *in vitro* (Kallies et al., 2007) and identified
148 population subsets in which *Jchain* expression precedes that of IRF4 and BLIMP1. The data also
149 demonstrated that increased levels of *Jchain* promoter-driven GFP expression correlates highly with
150 cells expressing critical plasma cell transcription factors supporting the observations made using cell
151 surface markers (**Fig. 2**).
152
153 ***Igjcre$^{ERT2(GFP)}$* mediated cre recombination is effective only in plasma cells**
154 We next sought to determine whether the *Igjcre$^{ERT2(GFP)}$* could be used to perform genetic manipulation
155 of plasma cells. We generated compound mutant mice carrying the *Igjcre$^{ERT2(GFP)}$* allele and a Rosa 26
156 allele in which RFP expression is conditional to cre-mediated recombination of a loxP-STOP-loxP
157 cassette (*R26^{lslRFP}*; (Luche et al., 2007)). In the *Igjcre$^{ERT2(GFP)}$* cre is fused to an estrogen binding domain
158 (ERT2) that sequesters cre in the cytoplasm through the binding to HSP90 (Feil et al., 2009) . Addition
159 of tamoxifen to the system displaces the cre^{ERT2}-HSP90 complex effectively allowing nuclear import of
160 cre^{ERT2} and its access to loxP flanked DNA sequences (Feil et al., 2009). We first performed an *in vitro*
161 experiment using a classical plasmablast (B220^{low}CD138^{+}) differentiation assay in which B cells
162 purified from mice carrying the *Igjcre$^{ERT2(GFP)}$* and *R26^{lslRFP}* alleles were cultured with LPS in the
163 presence or absence of 4-OH tamoxifen (Andersson et al., 1972). GFP expression was highly enriched
164 in plasmablasts compared to B cells and RFP expression was only observed upon addition of 4-OH
165 tamoxifen to the culture, and that occurred virtually only in plasmablasts (**Fig. S2**). This data suggests
166 that cre^{ERT2} was mostly induced in plasmablasts and was effectively retained in the cytoplasm in the
167 absence of 4-OH tamoxifen. Similar observations were made in mice carrying the *Igjcre$^{ERT2(GFP)}$* and
168 *R26^{lslRFP}* alleles *in vivo* in that absence of tamoxifen administration RFP expressing cells were not

169 detected, confirming the *in vitro* results and supporting that the *Igjcre*$^{ERT2(GFP)}$ allele was not "leaky" in
170 the control of cre activity (**Fig. S1B**, **C** and **E**). We next immunized mice carrying *Igjcre*$^{ERT2(GFP)}$ and
171 *R26*^{lslRFP} alleles and administered tamoxifen on days 7, 8, 9 and 10 followed by analysis of spleen and
172 bone marrow at day 12 (**Fig. 4A**). Analyses of the populations defined by varied GFP and B220 surface
173 expression (**Fig. 2 and 4B**) revealed that a small fraction of GFP^{low}B220^{high} cells were positive for RFP
174 in the spleen (median ~2%) and in the bone marrow (median ~1.2%; **Fig. 4C**). In contrast, cre mediated
175 recombination and as consequence RFP expression occurred in ~37% and ~31% of GFP^{int}B220^{int} in the
176 spleen and bone marrow, respectively, whereas the vast majority of cells within the GFP^{high}B220^{low}
177 population had undergone cre mediated recombination and were RFP positive (~76% in the spleen, and
178 ~88% in the bone marrow, median; **Fig. 4C** and **D**). These data showed that *Igjcre*$^{ERT2(GFP)}$ mediated cre
179 recombination was only effective in plasma cell populations and validated *Igjcre*$^{ERT2(GFP)}$ as a tool to
180 specifically perform genetic manipulation of plasma cells.
181
182 **Genetic manipulation using *Igjcre*$^{ERT2(GFP)}$ in plasma cells occurs across immunoglobulin isotypes**
183 IgG1 does not multimerize, and due to differences in its secretory tail to that of IgA and IgM, JCHAIN
184 does not associate with IgG1 (Johansen et al., 2000). It is currently assumed that *Jchain* expression
185 occurs in all plasma cells regardless of isotype, however, this has not been demonstrated at the single
186 cell level (Castro and Flajnik, 2014; Johansen et al., 2000; Mather et al., 1981). We performed
187 experiments that investigated whether *Igjcre*$^{ERT2(GFP)}$ allele GFP expression (as proxy for *Jchain*), and
188 cre-mediated loxP recombination occurred in plasma cells across immunoglobulin isotypes. For that
189 we analyzed the spleen, mLN, peyer's patches of younger (15 weeks) and older (30 weeks) mice
190 carrying the *Igjcre*$^{ERT2(GFP)}$ and *R26*^{lslRFP} alleles. These mice were immunized and administered with
191 tamoxifen on days 7, 8, 9 and 10 followed by analysis at day 12 (**Fig. 5A**). We first gated on total
192 plasma cells (B220^{low}CD138^{+}), and then on total GFP^{+} cells (RFP^{+} and RFP^{neg}, i.e. *Jchain* expressing)
193 and after that on GFP^{+}RFP^{+} cells (i.e. cre recombined) and determined the proportions of IgA, IgM and
194 IgG1 expressing cells within the plasma cell population and subpopulations using intracellular stain
195 (**Fig. 5B-D**). Analysis of spleens of 15-week-old mice revealed a slightly increased representation of
196 IgA^{+} cells within the GFP^{+}RFP^{+} plasma cells only when compared to total plasma cells (**Fig. 5E**). A

197 similar observation was made when analyzing the peyer's patches of 15-week-old mice (**Fig. 5E**).
198 However, for 15-week-old mice we did not observe differences in the representation of IgA in any of
199 the other tissues analyzed, and in none of the tissues for IgM and IgG1 (**Fig. 5E**). Analysis of 30-week-
200 old mice showed a slightly increased representation of IgM^+ cells within the GFP^+RFP^+ plasma cells
201 only when compared to total plasma cells, and for IgA^+ in mesenteric lymph node (mLN; **Fig. 5F**).
202 Nevertheless, for 30-week-old mice we did not observe a significant difference in the representation of
203 IgM or IgA in any of the other tissues analyzed, and in none of the tissues for IgG1 (**Fig. 5F**). Taken
204 together, these data suggested that *Jchain* expression is not overly represented in IgA or IgM expressing
205 plasma cells compared to $IgG1^+$ plasma cells. As consequence, only minor differences were observed
206 for $Igjcre^{ERT2(GFP)}$ mediated cre-loxP recombination across immunoglobulin isotypes indicating that the
207 $Igjcre^{ERT2(GFP)}$ is useful for genetic manipulation also of plasma cells expressing IgG1.
208

209 **$Igjcre^{ERT2(GFP)}$ allows lifespan studies and to trace long-lived plasma cells**

210 The lifespan of plasma cells has been a matter of debate and investigation for over 70 years (Manz and
211 Radbruch, 2002). This knowledge is important as it directly relates to long-term protection from
212 infection and could provide valuable information to improve vaccines. Multiple analyses using
213 primarily BrdU labeling pulse-chase experiments have generated conflicting results with some studies
214 suggesting a 3-week lifespan for a plasma cell and others more than 3 months (Ho et al., 1986; Manz
215 et al., 1997). These experiments have also showed that the half-life of plasma cells differs between
216 spleen and the bone marrow (Sze et al., 2000). We investigated the suitability of the $Igjcre^{ERT2(GFP)}$ allele
217 to determine the lifespan of plasma cells in the spleen and bone marrow. We immunized mice carrying
218 $Igjcre^{ERT2(GFP)}$ and $R26^{lslRFP}$ alleles at two time-points spaced by a period of 21 days (**Fig. 6A**, (Calado
219 et al., 2010)). Thirty days after the secondary immunization (day 51) we administered tamoxifen for 5
220 consecutive days to genetically label plasma cells (**Fig. 6A**). Next we determined genetically labelled
221 GFP^+RFP^+ plasma cells present in the spleen and bone marrow at day 5, and after 2 and 5 months after
222 the last tamoxifen administration (**Fig. 6B** and **C**). Compared to day 5, in which ~70% (median) of
223 $CD138^+CXCR4^+$ plasma cells in spleen and bone marrow were GFP^+RFP^+, that fraction was
224 significantly reduced in spleen and bone marrow at two months and more so at five months after the

225 last tamoxifen injection (**Fig. 6B** and **C**). As expected, with the generation of new plasma cells over
226 time, the opposite was true for the fraction of $GFP^{+}RFP^{neg}$ plasma cells (**Fig. 6B** and **C**). Remarkably,
227 by five months the reduction in the fraction of $GFP^{+}RFP^{+}$ plasma cells was more pronounced in the
228 spleen compared to the bone marrow (**Fig. 6B** and **C**). Still the data indicated that ~6.4% of plasma
229 cells in the spleen and ~16.4% in the bone marrow lived for at least 5 months (**Fig. 6B** and **C**). We next
230 calculated the half-life of plasma cells in the spleen and bone marrow. Consistent with the sharper
231 decrease of genetically labelled $GFP^{+}RFP^{+}$ plasma cells in the spleen over time, splenic GFP+RFP+
232 plasma cells displayed a calculated half-life of ~49.5 days, whereas that of $GFP^{+}RFP^{+}$ plasma cells in
233 the bone marrow was ~86.4 days. Notably the calculated half-life of genetically labelled plasma cells
234 in the bone marrow was consistent with BrdU labeling pulse-chase experiments suggesting that a
235 fraction of plasma cells survives for at least 3 months (Manz et al., 1997). These data demonstrated the
236 suitability of *Igjcre*$^{ERT2(GFP)}$ in time-stamping plasma cells using the expression of a fluorescent marker
237 and to identify long-lived plasma cells.
238
239
240
241
242
243
244
245
246
247
248
249
250
251
252

253 **Discussion**

254 Plasma cells are an essential component of the adaptive immune system. However, compared to other
255 B cell lineage populations, the molecular analysis of gene function *in vivo* as lagged behind. One
256 underlying cause is the lack of tools for specific genetic manipulation, something available for B cells
257 since 1997, more than 20 years ago (Rickert et al., 1997), and recently for B cells at multiple stages of
258 development (Boross et al., 2009; Casola et al., 2006; Croker et al., 2004; Crouch et al., 2007; de Boer
259 et al., 2003; Dogan et al., 2009; Duber et al., 2009; Georgiades et al., 2002; Hobeika et al., 2006; Kraus
260 et al., 2004; Kwon et al., 2008; Moriyama et al., 2014; Robbiani et al., 2008; Schweighoffer et al., 2013;
261 Shinnakasu et al., 2016; Weber et al., 2019; Yasuda et al., 2013).

262

263 Here we used a systematic analysis of developmental factors for which expression is increased during
264 plasma cell differentiation (*Xbp1*, *Jchain*, *Scd1*, *Irf4*, and *Prdm1*) to identify suitable candidates for the
265 generation of plasma cell-specific tools. *Blimp1*, the critical transcription factor for the establishment
266 of the plasma cell program, displayed an expression pattern unspecific to plasma cells. This was
267 unsurprising given the knowledge that *Blimp1* is expressed by other hematopoietic and non-
268 hematopoietic cells (John and Garrett-Sinha, 2009), including germ cells (Ohinata et al., 2005).
269 Amongst the analyzed factors we found *Jchain* to be the one with the highest RNA expression level in
270 plasma cells and the most plasma cell-specific expression pattern. We therefore considered *Jchain* to
271 be the most suitable candidate for the generation of plasma cell-specific tools.

272

273 We searched alleles generated by the EUCOMMTools consortium and identified a *Jchain* allele:
274 *Igjcre*$^{ERT2(GFP)}$and tested its functionally. Through a series of experiments, we characterized this allele
275 and demonstrated its suitability for specific genetic manipulation of plasma cells. Briefly, although
276 *Jchain* was expressed in a small subset of B cells (primarily GC B cells) and preceded BLIMP1 and
277 IRF4 expression, *Igjcre*$^{ERT2(GFP)}$ mediated cre recombination was only effective in plasma cells. In the
278 *Igjcre*$^{ERT2(GFP)}$ allele GFP and cre^{ERT2} are linked by a self-cleaving 2A peptide which ensures a near
279 equitable co-expression of the proteins (Szymczak et al., 2004). As consequence, it is likely that
280 effectiveness of cre recombination is relatable to the level of cre^{ERT2} because plasma cells expressed the

281 highest level of *Jchain*, as suggested by the GFP expression. Of note, the *Igjcre*$^{ERT2(GFP)}$ allele analyzed
282 in this work retained the puromycin selection cassette that is flanked by Rox recombination sites. This
283 knowledge should be taken in consideration in future experiments involving compound mutant mice
284 that make use of Dre recombinase (Anastassiadis et al., 2009). On occasion it has been observed that
285 retention of the selection cassette reduces gene expression of the targeted locus (Meyers et al., 1998;
286 Nagy et al., 1998). As consequence removal of the selection may potentially increase cre^{ERT2} expression,
287 including in B cells, and reduce the specificity of *Igjcre*$^{ERT2(GFP)}$ cre-mediated recombination to plasma
288 cells. Lastly in the *Igjcre*$^{ERT2(GFP)}$ allele the expression of *Jchain* is interrupted by a GFP-2A-creERT2
289 cassette and induction of cre-mediated recombination deletes *Jchain* exon 2 that is loxP-flanked. It was
290 previously shown that heterozygous deletion of *Jchain* displayed an intermediate phenotype to that of
291 knockout mice (Lycke et al., 1999). This knowledge must be taken into consideration when performing
292 *Igjcre*$^{ERT2(GFP)}$ cre-mediated genetic manipulation, including the need to use the *Igjcre*$^{ERT2(GFP)}$ allele
293 without the targeted manipulation as control, and the utility of the *Igjcre*$^{ERT2(GFP)}$ allele in homozygosity.
294 Future iterations of the *Igjcre*$^{ERT2(GFP)}$ in which JCHAIN protein expression is preserved should be
295 considered.
296
297 Previous analysis of *in vitro* cultures of *Blimp1* deficient B cells showed that initiation of *Jchain*
298 expression does not require BLIMP1 (Kallies et al., 2007). However, *Jchain* expression is higher in
299 BLIMP1 expressing cells (Kallies et al., 2007). We used the *Igjcre*$^{ERT2(GFP)}$ allele and identified a
300 population of cells *in vivo* marked by low GFP expression and high surface expression of B220
301 (GFP^{low}B220^{hi}) where only ~7% of cells expressed BLIMP1. It is thus possible that the GFP^{low}B220^{hi}
302 population identified in mice carrying the *Igjcre*$^{ERT2(GFP)}$ allele contains BLIMP1^{neg} plasma cell
303 precursor cells and future in-depth analysis may provide information on the mechanisms underlying the
304 very first steps of plasma cell differentiation.
305
306 It is generally assumed that *Jchain* expression occurs in all plasma cells regardless of their isotypes
307 (Castro and Flajnik, 2014; Johansen et al., 2000; Mather et al., 1981). The analysis performed in this
308 work using the *Igjcre*$^{ERT2(GFP)}$ allele confirmed at the single cell level that *Jchain* expression occurs in

309 plasma cells across immunoglobulin isotypes. However, given that in mice carrying the *Igjcre*$^{ERT2(GFP)}$
310 allele not all plasma cells expressed GFP, it did not support the concept *Jchain* is expressed by all
311 plasma cells. It is, however, necessary to consider that these analysis measure GFP expression that is
312 under the activity of the *Jchain* promoter, rather than JCHAIN directly.
313
314 We also demonstrated that the *Igjcre*$^{ERT2(GFP)}$ allele is a useful tool to study plasma cell life-span and to
315 identify long-lived plasma cells. Until now, most studies aiming to determine plasma cell longevity
316 have relied on BrdU or EdU labeling pulse-chase experiments (Ho et al., 1986; Lemke et al., 2016;
317 Manz et al., 1997). There are key differences between the genetic and the BrdU/EdU time-stamping
318 methods. The former labels existing plasma cells independently of when these cells were generated and
319 even if labelled cells were to undergo cell cycle the genetic mark would be maintained. On other hand,
320 BrdU or EdU labelling pulse-chase experiments are strictly dependent on cell cycle and therefore more
321 accurately mark the time at which plasma cells were generated, however, if division occurs in the
322 plasma cell pool the label may be lost. Still, the calculated half-life of plasma cells using the
323 *Igjcre*$^{ERT2(GFP)}$ allele was similar to that of some EdU or BrdU labelling studies (Lemke et al., 2016;
324 Manz et al., 1997). Where the *Igjcre*$^{ERT2(GFP)}$ allele will supersede BrdU labelling technologically is on
325 the ability to retrieve time-stamped live plasma cells at multiple time-points for downstream analysis.
326 That property can easily be combined with further genetic manipulation to investigate gene function,
327 paving the way for in-depth mechanistic understanding of physiology and pathology of plasma cells in
328 in vivo and in their niche.
329
330
331
332
333
334
335
336

Acknowledgments

We thank the members of the Immunity and Cancer laboratory (FCI, London) for critical discussions and review of the manuscript; the FCI BRF and Flow-cytometry platforms for expert advice and technical support.

This work was supported by The Francis Crick Institute which receives its core funding from Cancer Research UK (FC001057), the UK Medical Research Council (FC001057), and the Wellcome Trust (FC001057) to D.P.C., an MRC career development award MR/J008060/1 to D.P.C.

The authors declare no competing financial interests**.**

Author contributions: Conceptualization, A.Q.X., R.R.B, D.P.C.; Methodology, A.Q.X., R.R.B, D.P.C.; Investigation, A.Q.X., R.R.B, D.P.C.; Resources, D.P.C.; Writing – Original Draft, A.Q.X., and D.P.C.; Supervision D.P.C.; Funding Acquisition, D.P.C.

365 **References**

366 Alugupalli, K.R., J.M. Leong, R.T. Woodland, M. Muramatsu, T. Honjo, and R.M. Gerstein. 2004. B1b
367 lymphocytes confer T cell-independent long-lasting immunity. *Immunity* 21:379-390.
368 Anastassiadis, K., J. Fu, C. Patsch, S. Hu, S. Weidlich, K. Duerschke, F. Buchholz, F. Edenhofer, and
369 A.F. Stewart. 2009. Dre recombinase, like Cre, is a highly efficient site-specific recombinase
370 in E. coli, mammalian cells and mice. *Dis Model Mech* 2:508-515.
371 Andersson, J., O. Sjoberg, and G. Moller. 1972. Induction of immunoglobulin and antibody synthesis
372 in vitro by lipopolysaccharides. *Eur J Immunol* 2:349-353.
373 Bonami, R.H., W.T. Wolfle, J.W. Thomas, and P.L. Kendall. 2014. NFATc2 (NFAT1) assists BCR-
374 mediated anergy in anti-insulin B cells. *Mol Immunol* 62:321-328.
375 Boross, P., C. Breukel, P.F. van Loo, J. van der Kaa, J.W. Claassens, H. Bujard, K. Schonig, and J.S.
376 Verbeek. 2009. Highly B lymphocyte-specific tamoxifen inducible transgene expression of
377 CreER T2 by using the LC-1 locus BAC vector. *Genesis* 47:729-735.
378 Brandtzaeg, P., and H. Prydz. 1984. Direct evidence for an integrated function of J chain and secretory
379 component in epithelial transport of immunoglobulins. *Nature* 311:71-73.
380 Calado, D.P., B. Zhang, L. Srinivasan, Y. Sasaki, J. Seagal, C. Unitt, S. Rodig, J. Kutok, A.
381 Tarakhovsky, M. Schmidt-Supprian, and K. Rajewsky. 2010. Constitutive canonical NF-
382 kappaB activation cooperates with disruption of BLIMP1 in the pathogenesis of activated B
383 cell-like diffuse large cell lymphoma. *Cancer Cell* 18:580-589.
384 Casola, S., G. Cattoretti, N. Uyttersprot, S.B. Koralov, J. Seagal, Z. Hao, A. Waisman, A. Egert, D.
385 Ghitza, and K. Rajewsky. 2006. Tracking germinal center B cells expressing germ-line
386 immunoglobulin gamma1 transcripts by conditional gene targeting. *Proc Natl Acad Sci U S A*
387 103:7396-7401.
388 Castro, C.D., and M.F. Flajnik. 2014. Putting J chain back on the map: how might its expression define
389 plasma cell development? *J Immunol* 193:3248-3255.
390 Croker, B.A., D. Metcalf, L. Robb, W. Wei, S. Mifsud, L. DiRago, L.A. Cluse, K.D. Sutherland, L.
391 Hartley, E. Williams, J.G. Zhang, D.J. Hilton, N.A. Nicola, W.S. Alexander, and A.W. Roberts.
392 2004. SOCS3 is a critical physiological negative regulator of G-CSF signaling and emergency
393 granulopoiesis. *Immunity* 20:153-165.
394 Crouch, E.E., Z. Li, M. Takizawa, S. Fichtner-Feigl, P. Gourzi, C. Montano, L. Feigenbaum, P. Wilson,
395 S. Janz, F.N. Papavasiliou, and R. Casellas. 2007. Regulation of AID expression in the immune
396 response. *J Exp Med* 204:1145-1156.
397 de Boer, J., A. Williams, G. Skavdis, N. Harker, M. Coles, M. Tolaini, T. Norton, K. Williams, K.
398 Roderick, A.J. Potocnik, and D. Kioussis. 2003. Transgenic mice with hematopoietic and
399 lymphoid specific expression of Cre. *Eur J Immunol* 33:314-325.
400 Dogan, I., B. Bertocci, V. Vilmont, F. Delbos, J. Megret, S. Storck, C.A. Reynaud, and J.C. Weill. 2009.
401 Multiple layers of B cell memory with different effector functions. *Nat Immunol* 10:1292-1299.
402 Duber, S., M. Hafner, M. Krey, S. Lienenklaus, B. Roy, E. Hobeika, M. Reth, T. Buch, A. Waisman,
403 K. Kretschmer, and S. Weiss. 2009. Induction of B-cell development in adult mice reveals the
404 ability of bone marrow to produce B-1a cells. *Blood* 114:4960-4967.
405 Feil, S., N. Valtcheva, and R. Feil. 2009. Inducible Cre mice. *Methods Mol Biol* 530:343-363.
406 Georgiades, P., S. Ogilvy, H. Duval, D.R. Licence, D.S. Charnock-Jones, S.K. Smith, and C.G. Print.
407 2002. VavCre transgenic mice: a tool for mutagenesis in hematopoietic and endothelial lineages.
408 *Genesis* 34:251-256.
409 Hargreaves, D.C., P.L. Hyman, T.T. Lu, V.N. Ngo, A. Bidgol, G. Suzuki, Y.R. Zou, D.R. Littman, and
410 J.G. Cyster. 2001. A coordinated change in chemokine responsiveness guides plasma cell
411 movements. *J Exp Med* 194:45-56.
412 Heng, T.S., M.W. Painter, and C. Immunological Genome Project. 2008. The Immunological Genome
413 Project: networks of gene expression in immune cells. *Nat Immunol* 9:1091-1094.
414 Ho, F., J.E. Lortan, I.C. MacLennan, and M. Khan. 1986. Distinct short-lived and long-lived antibody-
415 producing cell populations. *Eur J Immunol* 16:1297-1301.
416 Hobeika, E., S. Thiemann, B. Storch, H. Jumaa, P.J. Nielsen, R. Pelanda, and M. Reth. 2006. Testing
417 gene function early in the B cell lineage in mb1-cre mice. *Proc Natl Acad Sci U S A* 103:13789-
418 13794.

419 Johansen, F.E., R. Braathen, and P. Brandtzaeg. 2000. Role of J chain in secretory immunoglobulin
420 formation. *Scand J Immunol* 52:240-248.
421 John, S.A., and L.A. Garrett-Sinha. 2009. Blimp1: a conserved transcriptional repressor critical for
422 differentiation of many tissues. *Exp Cell Res* 315:1077-1084.
423 Kallies, A., J. Hasbold, K. Fairfax, C. Pridans, D. Emslie, B.S. McKenzie, A.M. Lew, L.M. Corcoran,
424 P.D. Hodgkin, D.M. Tarlinton, and S.L. Nutt. 2007. Initiation of plasma-cell differentiation is
425 independent of the transcription factor Blimp-1. *Immunity* 26:555-566.
426 Klein, U., S. Casola, G. Cattoretti, Q. Shen, M. Lia, T. Mo, T. Ludwig, K. Rajewsky, and R. Dalla-
427 Favera. 2006. Transcription factor IRF4 controls plasma cell differentiation and class-switch
428 recombination. *Nat Immunol* 7:773-782.
429 Kraus, M., M.B. Alimzhanov, N. Rajewsky, and K. Rajewsky. 2004. Survival of resting mature B
430 lymphocytes depends on BCR signaling via the Igalpha/beta heterodimer. *Cell* 117:787-800.
431 Kwon, K., C. Hutter, Q. Sun, I. Bilic, C. Cobaleda, S. Malin, and M. Busslinger. 2008. Instructive role
432 of the transcription factor E2A in early B lymphopoiesis and germinal center B cell
433 development. *Immunity* 28:751-762.
434 Lemke, A., M. Kraft, K. Roth, R. Riedel, D. Lammerding, and A.E. Hauser. 2016. Long-lived plasma
435 cells are generated in mucosal immune responses and contribute to the bone marrow plasma
436 cell pool in mice. *Mucosal Immunol* 9:83-97.
437 Luche, H., O. Weber, T. Nageswara Rao, C. Blum, and H.J. Fehling. 2007. Faithful activation of an
438 extra-bright red fluorescent protein in "knock-in" Cre-reporter mice ideally suited for lineage
439 tracing studies. *Eur J Immunol* 37:43-53.
440 Lycke, N., L. Erlandsson, L. Ekman, K. Schon, and T. Leanderson. 1999. Lack of J chain inhibits the
441 transport of gut IgA and abrogates the development of intestinal antitoxic protection. *J Immunol*
442 163:913-919.
443 Manz, R.A., and A. Radbruch. 2002. Plasma cells for a lifetime? *Eur J Immunol* 32:923-927.
444 Manz, R.A., A. Thiel, and A. Radbruch. 1997. Lifetime of plasma cells in the bone marrow. *Nature*
445 388:133-134.
446 Mather, E.L., F.W. Alt, A.L. Bothwell, D. Baltimore, and M.E. Koshland. 1981. Expression of J chain
447 RNA in cell lines representing different stages of B lymphocyte differentiation. *Cell* 23:369-
448 378.
449 Max, E.E., and S.J. Korsmeyer. 1985. Human J chain gene. Structure and expression in B lymphoid
450 cells. *J Exp Med* 161:832-849.
451 Meyers, E.N., M. Lewandoski, and G.R. Martin. 1998. An Fgf8 mutant allelic series generated by Cre-
452 and Flp-mediated recombination. *Nat Genet* 18:136-141.
453 Moriyama, S., N. Takahashi, J.A. Green, S. Hori, M. Kubo, J.G. Cyster, and T. Okada. 2014.
454 Sphingosine-1-phosphate receptor 2 is critical for follicular helper T cell retention in germinal
455 centers. *J Exp Med* 211:1297-1305.
456 Nagy, A., C. Moens, E. Ivanyi, J. Pawling, M. Gertsenstein, A.K. Hadjantonakis, M. Pirity, and J.
457 Rossant. 1998. Dissecting the role of N-myc in development using a single targeting vector to
458 generate a series of alleles. *Curr Biol* 8:661-664.
459 Nutt, S.L., P.D. Hodgkin, D.M. Tarlinton, and L.M. Corcoran. 2015. The generation of antibody-
460 secreting plasma cells. *Nat Rev Immunol* 15:160-171.
461 Ohinata, Y., B. Payer, D. O'Carroll, K. Ancelin, Y. Ono, M. Sano, S.C. Barton, T. Obukhanych, M.
462 Nussenzweig, A. Tarakhovsky, M. Saitou, and M.A. Surani. 2005. Blimp1 is a critical
463 determinant of the germ cell lineage in mice. *Nature* 436:207-213.
464 Palumbo, A., and K. Anderson. 2011. Multiple myeloma. *N Engl J Med* 364:1046-1060.
465 Pracht, K., J. Meinzinger, P. Daum, S.R. Schulz, D. Reimer, M. Hauke, E. Roth, D. Mielenz, C. Berek,
466 J. Corte-Real, H.M. Jack, and W. Schuh. 2017. A new staining protocol for detection of murine
467 antibody-secreting plasma cell subsets by flow cytometry. *Eur J Immunol* 47:1389-1392.
468 Rickert, R.C., J. Roes, and K. Rajewsky. 1997. B lymphocyte-specific, Cre-mediated mutagenesis in
469 mice. *Nucleic Acids Res* 25:1317-1318.
470 Rinkenberger, J.L., J.J. Wallin, K.W. Johnson, and M.E. Koshland. 1996. An interleukin-2 signal
471 relieves BSAP (Pax5)-mediated repression of the immunoglobulin J chain gene. *Immunity*
472 5:377-386.

473 Robbiani, D.F., A. Bothmer, E. Callen, B. Reina-San-Martin, Y. Dorsett, S. Difilippantonio, D.J.
474 Bolland, H.T. Chen, A.E. Corcoran, A. Nussenzweig, and M.C. Nussenzweig. 2008. AID is
475 required for the chromosomal breaks in c-myc that lead to c-myc/IgH translocations. *Cell*
476 135:1028-1038.
477 Schweighoffer, E., L. Vanes, J. Nys, D. Cantrell, S. McCleary, N. Smithers, and V.L. Tybulewicz. 2013.
478 The BAFF receptor transduces survival signals by co-opting the B cell receptor signaling
479 pathway. *Immunity* 38:475-488.
480 Shaffer, A.L., M. Shapiro-Shelef, N.N. Iwakoshi, A.H. Lee, S.B. Qian, H. Zhao, X. Yu, L. Yang, B.K.
481 Tan, A. Rosenwald, E.M. Hurt, E. Petroulakis, N. Sonenberg, J.W. Yewdell, K. Calame, L.H.
482 Glimcher, and L.M. Staudt. 2004. XBP1, downstream of Blimp-1, expands the secretory
483 apparatus and other organelles, and increases protein synthesis in plasma cell differentiation.
484 *Immunity* 21:81-93.
485 Shapiro-Shelef, M., K.I. Lin, L.J. McHeyzer-Williams, J. Liao, M.G. McHeyzer-Williams, and K.
486 Calame. 2003. Blimp-1 is required for the formation of immunoglobulin secreting plasma cells
487 and pre-plasma memory B cells. *Immunity* 19:607-620.
488 Shinnakasu, R., T. Inoue, K. Kometani, S. Moriyama, Y. Adachi, M. Nakayama, Y. Takahashi, H.
489 Fukuyama, T. Okada, and T. Kurosaki. 2016. Regulated selection of germinal-center cells into
490 the memory B cell compartment. *Nat Immunol* 17:861-869.
491 Sze, D.M., K.M. Toellner, C. Garcia de Vinuesa, D.R. Taylor, and I.C. MacLennan. 2000. Intrinsic
492 constraint on plasmablast growth and extrinsic limits of plasma cell survival. *J Exp Med*
493 192:813-821.
494 Szymczak, A.L., C.J. Workman, Y. Wang, K.M. Vignali, S. Dilioglou, E.F. Vanin, and D.A. Vignali.
495 2004. Correction of multi-gene deficiency in vivo using a single 'self-cleaving' 2A peptide-
496 based retroviral vector. *Nat Biotechnol* 22:589-594.
497 Weber, T., J. Seagal, W. Winkler, T. Wirtz, V.T. Chu, and K. Rajewsky. 2019. A novel allele for
498 inducible Cre expression in germinal center B cells. *Eur J Immunol* 49:192-194.
499 Yasuda, T., T. Wirtz, B. Zhang, T. Wunderlich, M. Schmidt-Supprian, T. Sommermann, and K.
500 Rajewsky. 2013. Studying Epstein-Barr virus pathologies and immune surveillance by
501 reconstructing EBV infection in mice. *Cold Spring Harb Symp Quant Biol* 78:259-263.
502
503
504
505
506
507
508
509
510
511
512
513
514
515

516 **Figure legends**

517 **Figure 1. *Jchain* transcripts are highly enriched in plasma cell populations**.

518 **(A)** Schematic of the network of factors associated with plasma cell differentiation. Upwards arrows
519 indicate increased expression compared to the precursor population. **(B-D)** Differential gene
520 expression analysis using RNA sequencing data (ImmGen, (Heng et al., 2008)). (B) Analysis of *Xbp1*
521 and *Irf4*, which encode for XBP1 and IRF4, respectively. (C) Analysis of *Sdc1* and *Prdm1*, which
522 encode for CD138 and BLIMP1, respectively. (D) Analysis for *Jchain* (*Igj*) that encodes for
523 JCHAIN. "x" indicates fold change. Expression Value Normalized by DESeq2.
524 http://rstats.immgen.org/Skyline/skyline.html.

525

526 **Figure 2. *Jchain* is expressed in a small fraction of GC B cells and in most Plasma cells**.

527 **(A)** Schematic of *Jchain* targeted allele Wtsi MGI:5633773. Rectangular boxes indicate exons, and
528 exon number is on top; pink triangle indicates a FRT sequence; EGFPcre^{ERT2} cassette contains a splice
529 acceptor site (SA)-led EGFP-2A-creERT2 expression cassette followed by a poly-A tail inserted in the
530 intron between exons 1 and 2; white triangle indicates a ROX sequence; orange rectangle indicates a
531 promoter driven puromycin resistance cassette; green triangle indicates loxP sequence. **(B)** Schematic
532 of experimental procedure protocol. Mice carrying the *Igjcre$^{ERT2(GFP)}$* allele were immunized with sheep
533 red blood cells (SRBC) intravenously (i.v.) on day 0 and spleens of mice were analyzed at day 12 post-
534 immunization. **(C)** Gating strategy of populations by flow-cytometry according to the expression of
535 GFP and B220 in mice carrying the *Igjcre$^{ERT2(GFP)}$* allele and wild-type B6 mice for negative control of
536 GFP expression. **(D)** Gating strategy by flow-cytometry for plasma cells within the GFP^{hi}B220^{low}
537 population using CD138^{+} and CD138^{+}CXCR4^{+} markers. **(E)** Cumulative data for CD138^{+} and
538 CD138^{+}CXCR4^{+} plasma cells analyzed as in (D). Top: fraction of CD138^{+} plasma cells; Bottom:
539 fraction of CD138^{+}CXCR4^{+} plasma cells within the four populations defined by flow-cytometry
540 according to the expression of GFP and B220 in mice carrying the *Igjcre$^{ERT2(GFP)}$* allele. **(F)** Gating
541 strategy by flow-cytometry for total CD138^{+} and CD138^{+}CXCR4^{+} plasma cells within GFP^{low}B220^{hi}
542 population. The CD138^{neg} cell fraction within the GFP^{low}B220^{hi} population was analyzed for the CD19
543 B cell marker and stained for CD38 and FAS to determine germinal center (GC) B cells. **(G)** Cumulative

544 data for the frequency of GC B cells within the CD138^{neg}GFP^{low}B220^{hi} population. Each symbol (E, G)
545 represents an individual mouse; small horizontal lines indicate median, minimum and maximum values.
546 ***=p≤0.001, ****=p≤0.0001 (unpaired Student's *t*-test). Data are representative of three independent
547 experiments (E, G).
548
549 **Figure 3. *Jchain* precedes IRF4 and BLIMP1 expression**.
550 **(A)** Schematic of experimental procedure protocol. Mice carrying the *Igjcre$^{ERT2(GFP)}$* allele were
551 immunized with sheep red blood cells (SRBC) intravenously (i.v.) on day 0 and spleens of mice were
552 analyzed at day 12 post-immunization. **(B)** Gating strategy of populations by flow-cytometry according
553 to the expression of GFP and B220 in mice carrying the *Igjcre$^{ERT2(GFP)}$* allele. Wild-type B6 mice for
554 negative control of GFP expression. **(C)** Gating strategy for IRF4 and BLIMP1 expression by flow-
555 cytometry within the GFP^{neg}B220^{neg} population. **(D)** Gating strategy for IRF4 and BLIMP1 expression
556 by flow-cytometry within GFP^{low}B220^{hi}, GFP^{int}B220^{int} and GFP^{hi}B220^{low} populations, defined as in (B).
557 **(E)** Cumulative data for the frequency of BLIMP1^{+}IRF4^{+} cells within the four populations defined as
558 in (B). Each symbol in (E) represents an individual mouse; small horizontal lines indicate median,
559 minimum and maximum values. ns=not significant, ***=p≤0.001, ****=p≤0.0001 (unpaired Student's
560 *t*-test). Data are representative of three independent experiments (E).
561
562 **Figure 4. *Igjcre$^{ERT2(GFP)}$* mediated cre recombination is effective only in plasma cells**.
563 **(A)** Schematic of experimental procedure protocol. Mice carrying the *Igjcre$^{ERT2(GFP)}$* and *R26^{lslRFP}* alleles
564 were immunized with sheep red blood cells (SRBC) intravenously (i.v.) on day 0 and spleens (top) and
565 bone marrow (bottom) of mice were analyzed at day 12 post-immunization. A group of mice received
566 tamoxifen treatment for four consecutive days from day 7 to day 10 after immunization. **(B)** Gating
567 strategy of populations by flow-cytometry in spleen (top) and bone marrow (bottom) according to the
568 expression of GFP and B220 in mice carrying the *Igjcre$^{ERT2(GFP)}$* allele. Wild-type B6 mice for negative
569 control of GFP expression. **(C)** Gating strategy for GFP and RFP expression by flow-cytometry in the
570 four populations defined as in (B). Top: spleen; bottom: bone marrow. **(D)** Cumulative data for the

571 frequency and number of $GFP^{+}RFP^{+}$ cells within $GFP^{neg}B220^{neg}$, $GFP^{low}B220^{hi}$, $GFP^{int}B220^{int}$ and
572 $GFP^{hi}B220^{low}$ populations, defined as in (B). Top: spleen; bottom: bone marrow. Each symbol (D)
573 represents an individual mouse; small horizontal lines indicate median, minimum and maximum values.
574 ns=not significant, *=p≤0.05, **=p≤0.01, ***=p≤0.001, ****=p≤0.0001 (unpaired Student's *t*-test).
575 Data are representative of three independent experiments (D).
576
577 **Figure 5. Genetic manipulation using *Igjcre$^{ERT2(GFP)}$* occurs across immunoglobulin isotypes**.
578 **(A)** Schematic of experimental procedure protocol. Mice carrying the *Igjcre$^{ERT2(GFP)}$* and *R26^{lslRFP}* alleles
579 were immunized with sheep red blood cells (SRBC) intravenously (i.v.) on day 0 and spleens,
580 mesenteric lymph nodes (mLN), peyer's patches, and bone marrows of mice were analyzed at day 12
581 post-immunization. Mice received tamoxifen treatment for four consecutive days from day 7 to day 10
582 after immunization. **(B)** Gating strategy by flow-cytometry for intracellular and extracellular expression
583 of IgG1, IgM and IgA within total $B220^{low}CD138^{+}$ plasma cells. Analysis in the spleen is provided as
584 example. **(C)** Gating strategy by flow-cytometry for intracellular and extracellular expression of IgG1,
585 IgM and IgA within $B220^{low}CD138^{+}GFP^{+}$ (RFP^{+} and RFP^{neg}) plasma cells. Analysis in the spleen is
586 provided as example. **(D)** Gating strategy by flow-cytometry for intracellular and extracellular
587 expression of IgG1, IgM and IgA within $B220^{low}CD138^{+}GFP^{+}RFP^{+}$ plasma cells. Analysis in the spleen
588 is provided as example. **(E)** Cumulative data for the fractions of IgA, IgM or IgG1 expressing cells
589 within total plasma cells (PC) (black, $B220^{low}CD138^{+}$), GFP^{+} (RFP^{+} and RFP^{neg}) plasma cells (green,
590 $B220^{low}CD138^{+}GFP^{+}$), and $GFP^{+}RFP^{+}$ plasma cells (orange, $B220^{low}CD138^{+}GFP^{+}RFP^{+}$) at 15 weeks
591 of age. **(F)** Cumulative data for the fractions of IgA, IgM or IgG1 expressing cells within total plasma
592 cells (PC) (black, $B220^{low}CD138^{+}$), GFP^{+} (RFP^{+} and RFP^{neg}) plasma cells (green,
593 $B220^{low}CD138^{+}GFP^{+}$), and $GFP^{+}RFP^{+}$ plasma cells (orange, $B220^{low}CD138^{+}GFP^{+}RFP^{+}$) at 30 weeks
594 of age. Each symbol (E, F) represents an individual mouse; small horizontal lines indicate median,
595 minimum and maximum values. ns=not significant, *=p≤0.05 (2way ANOVA). Data are representative
596 of three independent experiments (E, F).
597

598 **Figure 6. *Igjcre$^{ERT2(GFP)}$* allows the study of plasma cell lifespan**.

599 **(A)** Schematic of experimental procedure protocol. Mice carrying the *Igjcre$^{ERT2(GFP)}$* and *R26^{lslRFP}* alleles
600 were immunized twice with sheep red blood cells (SRBC) intravenously (i.v.) on day 0 and day 21.
601 Mice received tamoxifen treatment for five consecutive days from day 51 to 55 after the first
602 immunization. Spleens and bone marrow of mice were analyzed at the five-day, two-month and five-
603 month timepoints after the last tamoxifen administration. **(B)** Cumulative data for the fraction of
604 GFP$^+$RFP$^+$ cells (left) and GFP$^+$RFP^{neg} cells (right) within CD138$^+$CXCR4$^+$ plasma cells in the spleen.
605 **(C)** Cumulative data for the fraction of GFP$^+$RFP$^+$ cells (left) and GFP$^+$RFP^{neg} cells (right) within
606 CD138$^+$CXCR4$^+$ plasma cells in the bone marrow. **(D)** Graphical representation of R^2 and half-life of
607 GFP$^+$RFP$^+$CD138$^+$CXCR4$^+$ plasma cells in the spleen using the data presented in (B). Graphing of best-
608 fit curve was performed using the GraphPad Prism 8 software. **(E)** Graphical representation of R^2 and
609 half-life of GFP$^+$RFP$^+$CD138$^+$CXCR4$^+$ plasma cells in the bone marrow using the data presented in
610 (B). Graphing of best-fit curve was performed using the GraphPad Prism 8 software. Each symbol (B,
611 C) represents an individual mouse; small horizontal lines indicate median, minimum and maximum
612 values. ns=not significant, *=p≤0.05 **=p≤0.01, ***=p≤0.001, ****=p≤0.0001 (unpaired Student's *t*-
613 test). Data are representative of three independent experiments (B, C).

614

615 **Supplemental Figure Legends**

616 **Figure S1. *Jchain* expression in multiple stages of B cell development and other cell lineages**

617 **(A)** Gating strategy by flow-cytometry for the B cell lineage in the spleen. Mice carrying the
618 *Igjcre$^{ERT2(GFP)}$* and *R26^{lslRFP}* alleles were immunized with sheep red blood cells (SRBC) intravenously
619 (i.v.) at day 0 and spleens were analyzed at day 12. Mice did not receive tamoxifen treatment. Cells
620 were pre-gated on live singlets and for the expression of CD138 and CXCR4 markers. CD138$^+$CXCR4$^+$
621 cells were defined as plasma cells (PC). Non-PCs positive for the CD19 and B220 markers were defined
622 as B2 cells, whereas those cells displaying a CD19$^+$B220^{low} were defined as B1 cells. B1 cells were
623 further characterized as B1a (CD5^{hi}CD23^{neg}) and B1b (CD5^{low}CD23^{neg}) cells. B2 cells were further
624 delineated into marginal zone (MZ) B cells (CD21^{hi}CD23^{int}), T1 B cells (CD21^{low}CD23^{low}), T2 B cells
625 (CD21^{int}IgM^{hi}CD23^{hi}) and Follicular B cells (Fo, CD21^{int}IgM^{int}CD23^{hi}. Non MZ or T1 cells were gated

626 for germinal center (GC) B cells ($CD38^{low}FAS^{high}$) and these were further delineated into dark zone GC
627 B cells ($CXCR4^{high}CD86^{low}$) and light zone GC B cells ($CXCR4^{low}CD86^{high}$). (Bonami et al., 2014) **(B)**
628 Cumulative data for fractions of $GFP^{+}RFP^{neg}$ and $GFP^{+}RFP^{+}$ cells within the B cell lineage in the spleen.
629 Analyzed as in (A). **(C)** Cumulative data for fractions of $GFP^{+}RFP^{neg}$ cells and $GFP^{+}RFP^{+}$ cells in
630 additional B cell lineage and non-B cell lineage populations in the spleen. Analyzed as in (A). **(D)**
631 Gating strategy by flow-cytometry for the B cell lineage in the bone marrow. Mice carrying the
632 *Igjcre*$^{ERT2(GFP)}$ and *R26*^{lslRFP} alleles were immunized with sheep red blood cells (SRBC) intravenously
633 (i.v.) at day 0 and spleens were analyzed at day 12. Mice did not receive tamoxifen treatment. Cells
634 were pre-gated on live singlets and gated for CD138 and B220 expression. $CD138^{+}B220^{low}$ cells were
635 defined as plasma cells (PCs) Non-PCs positive for the CD19 and B220 markers were further examined
636 and further delineated to immature B cells ($IgM^{+}CD43^{neg}$), Pre-B cells (fraction D; $IgM^{neg}CD43^{neg}$) and
637 Pro-B cells ($IgM^{neg}CD43^{+}$). Pro B cells were further sub-divided into Hardy fraction A ($BP1^{neg}CD24^{neg}$),
638 fraction B ($BP1^{neg}CD24^{+}$), fraction C ($BP1^{+}CD24^{neg}$) and fraction C' ($BP1^{+}CD24^{+}$). **(E)** Cumulative
639 data for fractions of $GFP^{+}RFP^{neg}$ cells and $GFP^{+}RFP^{+}$ cells in the B cell lineage and in plasma cells in
640 the bone marrow. Analyzed as in (D). Each symbol (B, C, E) represents an individual mouse; small
641 horizontal lines indicate median, minimum and maximum values. Data are representative of three
642 independent experiments (B, C, E).
643
644 **Figure S2. *Igjcre*$^{ERT2(GFP)}$ mediated recombination in vitro**.
645 (**A**) Gating strategy by flow-cytometry for GFP and RFP expression within $CD19^{+}B220^{+}$ B cells and
646 $B220^{low}CD138^{+}$ plasmablasts. Splenic B cells from unmanipulated mice carrying the *Igjcre*$^{ERT2(GFP)}$ and
647 *R26*^{lslRFP} alleles were enriched using CD43 negative depletion (MACS) and culture *in vitro* in the
648 presence of LPS and 4-hydroxytamoxifen (4-OH-TAM). Cells were analyzed 48h, 72h, and 96h time-
649 points for GFP and RFP expression by flow-cytometry. Data from 96h analysis of a B cell culture with
650 LPS and 1μM 4-OH-TAM is shown as example. (**B**) Cumulative data for fractions of $GFP^{neg}RFP^{neg}$,
651 $GFP^{+}RFP^{neg}$, $GFP^{+}RFP^{+}$ cells within B cells. Analyzed as in (A). (**C**) Cumulative data for fractions of
652 $GFP^{neg}RFP^{neg}$, $GFP^{+}RFP^{neg}$, $GFP^{+}RFP^{+}$ cells within plasmablasts. Analyzed as in (A).
653

654 **Materials and Methods**

655 **Mice:** The *Igjcre*$^{ERT2(GFP)}$ allele was purchased from EMMA in agreement with the Wellcome Trust
656 Sanger Institute (Jchain targeted allele Wtsi MGI:5633773, genebank https://www.i-
657 dcc.org/imits/targ_rep/alleles/43805/escell-clone-genbank-file) and mice were rederived at the
658 The Francis Crick Institute. The allele contains a splice acceptor site (SA), an *EGFP-2A-creERT2*
659 expression cassette and a poly-A tail in the intron between exons 1 and 2 under the *Jchain* promoter. In
660 addition, exon 2 is loxP-flanked and the allele also contains a Rox-flanked puromycin resistance
661 cassette. These mice were crossed to carry a *Rosa26*^{lsl}*RFP* cre recombination reporter allele (R26$^{lsl.RFP}$)
662 allele that expresses a non-toxic tandem-dimer red fluorescent protein upon cre-mediated deletion of a
663 floxed STOP cassette (Luche et al., 2007). Mice were maintained on the C57BL/6 background and bred
664 at The Francis Crick Institute biological resources facility under specific pathogen-free conditions.
665 Animal experiments were carried out in accordance with national and institutional guidelines for animal
666 care and were approved by The Francis Crick Institute biological resources facility strategic oversight
667 committee (incorporating the Animal Welfare and Ethical Review Body) and by the Home Office, UK.
668 All animal care and procedures followed guidelines of the UK Home Office according to the Animals
669 (Scientific Procedures) Act 1986 and were approved by Biological Research Facility at the Francis
670 Crick Institute. The age of mice ranged between 15-30 weeks as specified.

671

672 **Immunization and *in vivo* induction of cre activity**: Mice were injected intravenously with 1 x 10^9
673 sheep red blood cells (SRBCs, TCS Biosciences Ltd) in PBS. For the induction of cre activity, 4mg
674 tamoxifen (SIGMA T5648) dissolved in sunflower seed oil were administered by oral gavage to mice
675 once per day for multiple days depending on experimental design.

676

677 ***In vitro* B cell culture and induction cre activity**: Splenic cells were harvested and B cells were
678 isolated using CD43 (Ly-48) MicroBeads, mouse (Miltenyi Biotec). The purity of B cells was
679 determined by flow-cytometry (>95%). B cells were cultured in 96-well round-bottom plates (Falcon)
680 in B cell media in B cell media (DMEM high glucose/Glutamax from ThermoFisher Scientific

681 supplemented with 10% fetal bovine serum F7524 from Sigma, 100 U/mL Penicillin and 100 µg/mL
682 Streptomycin from Life Technologies, 10 mM HEPES Buffer Solution from Life Technologies, 100
683 µM MEM Non-essential Amino Acids from ThermoFisher Scientific, 1 mM sodium pyruvate from Life
684 Technologies and 50 uM β-mercaptoethanol from Sigma) at 1 million/mL concentration (200,000
685 cells/well) with 10ug/mL LPS and varied concentrations of (Z) 4-hydroxytamoxifen (Sigma-Aldrich).
686 Analysis was performed by flow-cytometry at 48, 72 or 96 hours of culture.
687
688 **Antibodies:** Rat Anti-Mouse Blimp-1, Clone 6D3 (BD Biosciences); Rat Anti-Mouse CD16/CD32,
689 Clone 2.4G2 (BD Biosciences); Rat Anti-Mouse CD19, Clone 1D3 (BD Biosciences); Rat Anti-Mouse
690 CD23, Clone B3B4 (BD Biosciences); Rat Anti-Mouse CD38, Clone 90 (BD Biosciences); Hamster
691 Anti-Mouse CD95, Clone Jo2 (BD Biosciences); Rat Anti-Mouse IgG1, Clone A85-1 (BD
692 Biosciences); Rat Anti-Mouse CD138, Clone 281-2 (BD Biosciences); Rat Anti-Mouse CD45R/B220,
693 Clone RA3-6B2 (BioLegend); Hamster Anti-Mouse CD11c, Clone N418 (BioLegend); Rat Anti-
694 Mouse CD19, Clone 6D5 (BioLegend); Rat Anti-Mouse CD21/35, Clone 7E9 (BioLegend); Rat Anti-
695 Mouse CD43, Clone 1B11 (BioLegend); Rat Anti-Mouse CD86, Clone GL1 (BioLegend); Rat Anti-
696 Mouse BP1, Clone 6C3 (eBioscience); Rat Anti-Mouse CD5, Clone 53-7.3 (eBioscience); Rat Anti-
697 Mouse CXCR4, Clone 2B11 (eBioscience); Rat Anti-Mouse IgA, Clone 11-44-2 (eBioscience); Rat
698 Anti-Mouse IgM, Clone II/41 (eBioscience); Rat Anti-mouse IRF4, Clone 3E4 (eBioscience).
699
700 **Flow cytometry**: Single cell suspensions were stained with antibodies. We used Zombie NIR Fixable
701 Viability Kit (BioLegend) for live/dead discrimination. For intracellular staining we fixed cells using
702 the BD CytoFix/Cytoperm (BD Biosciences) kit as per manufacturer instructions. Samples were
703 acquired on a BD LSRFortessa analyser using FACSDiva software (BD) and analysed on FlowJo
704 software.
705
706 **Quantification and statistical analysis:** Data were analyzed with unpaired two-tailed Student's t test
707 or 2way ANOVA; a p-value of 0.05 or less was considered significant. Prism (v7 and v8, GraphPad)
708 was used for statistical analysis. A single asterisk (*) in the graphs of figures represents a p-value ≤0.05,

709 double asterisks (**) a p-value ≤0.01, triple asterisks (***) a p-value ≤0.001, quadruple asterisks (****) a
710 p-value ≤0.0001, and "ns" stands for not statistically significant, i.e., a p-value >0.05.
711

712 **Online supplemental material:** Figure S1 displays the analysis of *Jchain* expression across cell
713 lineages in the spleen and bone marrow. These data also demonstrates that *Igjcre*$^{ERT2(GFP)}$ cre-mediated
714 recombination does not occur in the absence of tamoxifen treatment. Figure S1 shows experiments
715 using a classical LPS induced B to plasmablast differentiation and the occurrence of *Igjcre*$^{ERT2(GFP)}$ cre-
716 mediated recombination upon addition of increasing concentrations of 4-hydroxytamoxifen (4-OH-
717 TAM).

718

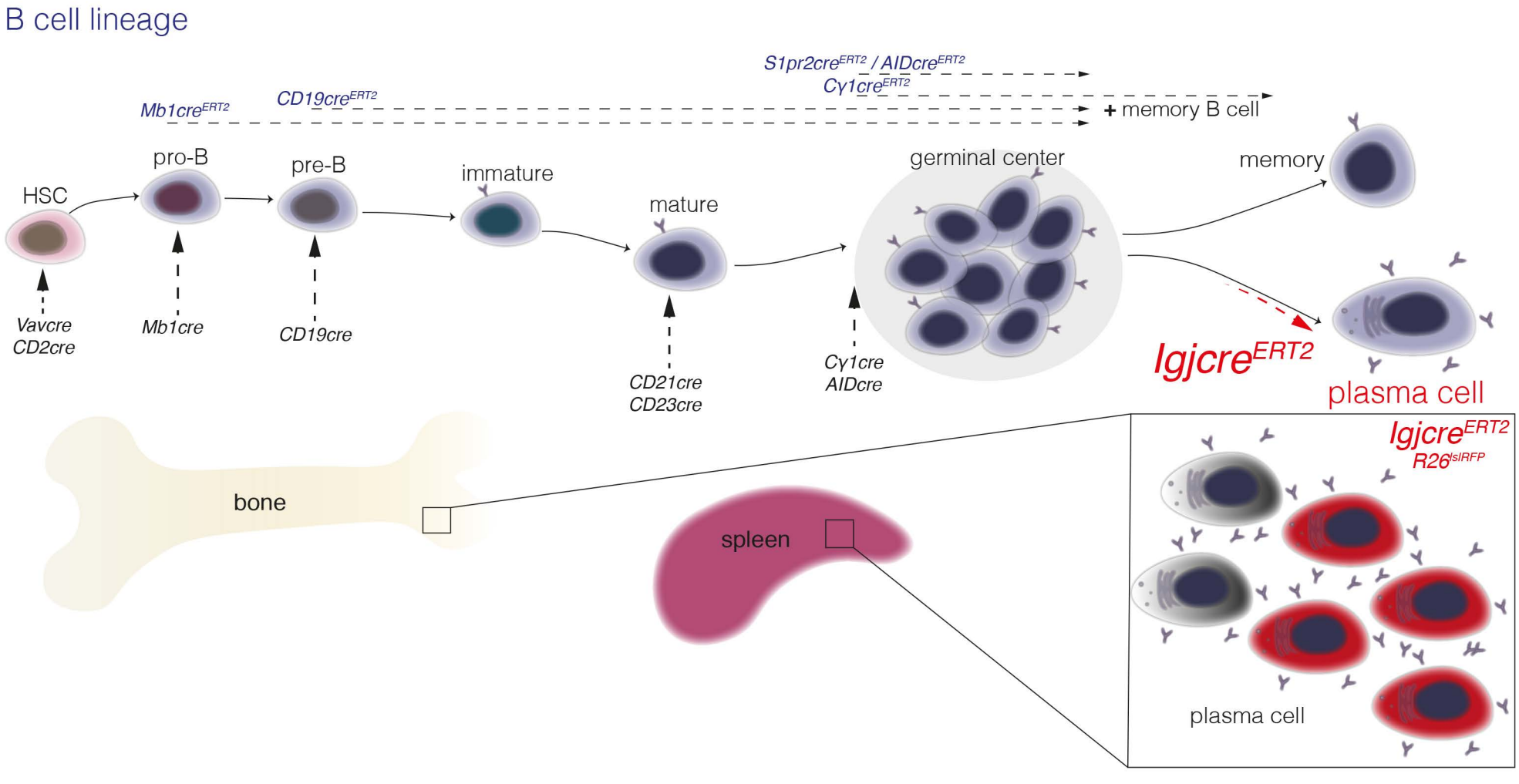

Xu A.Q. et al.

Graphical Abstract

Figure 1:

Jchain transcripts are highly enriched in plasma cell populations

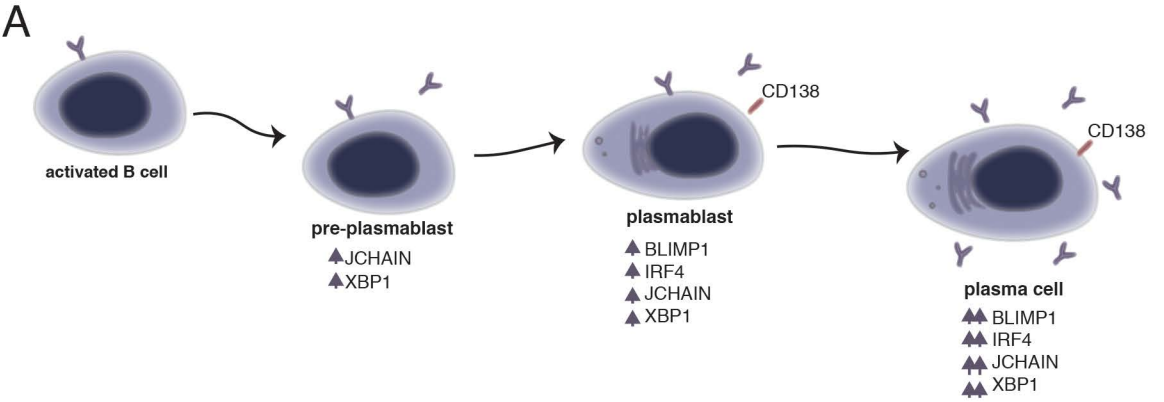

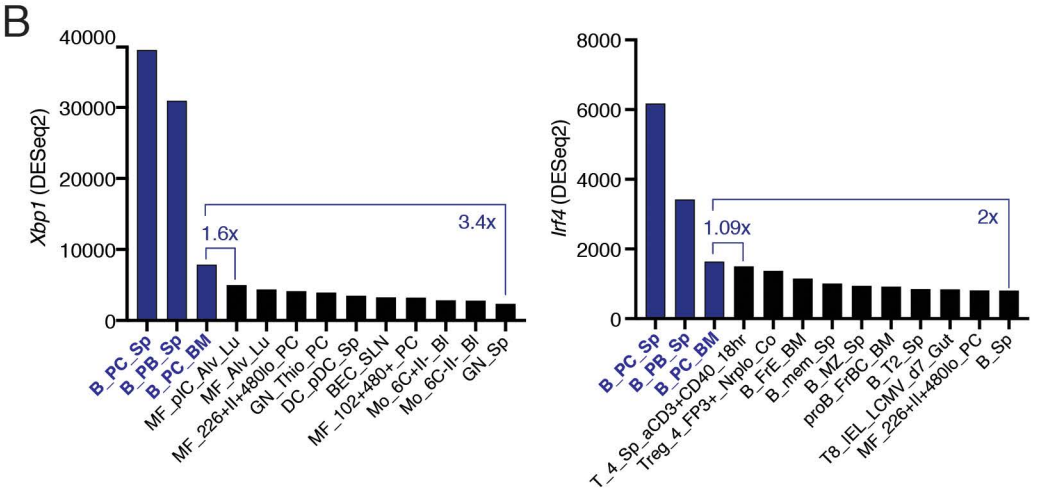

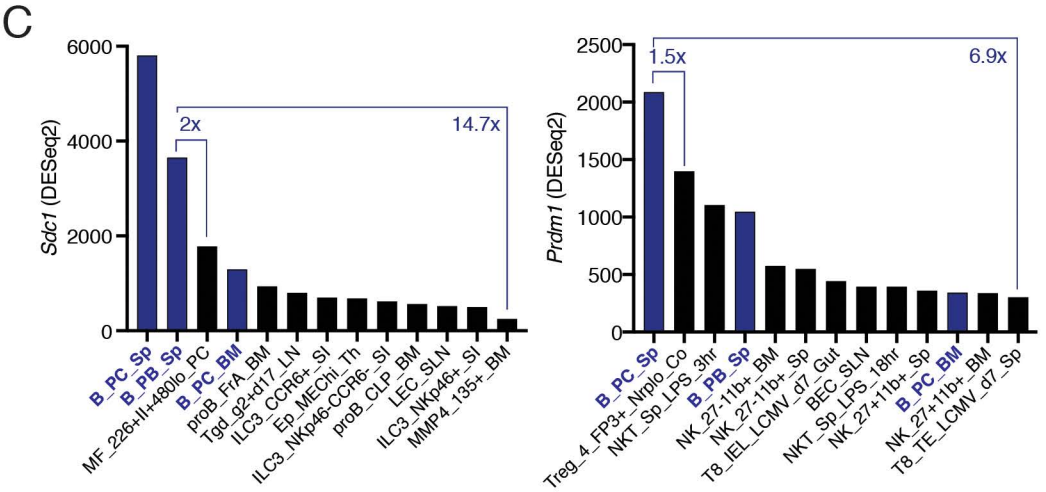

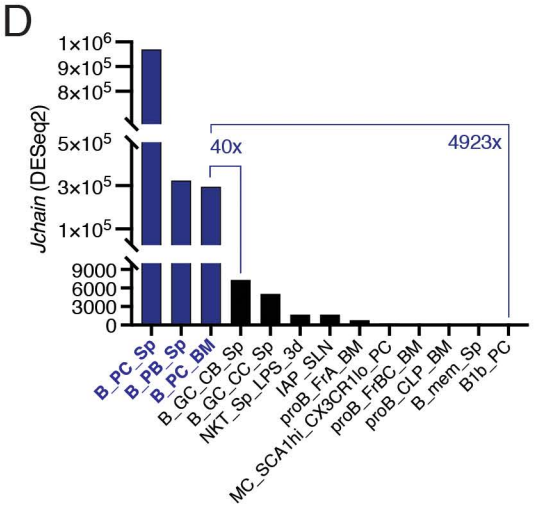

Xu A.Q. et al.

Figure 2.

Jchain is expressed in a small fraction of GC B cells and in most plasma cells

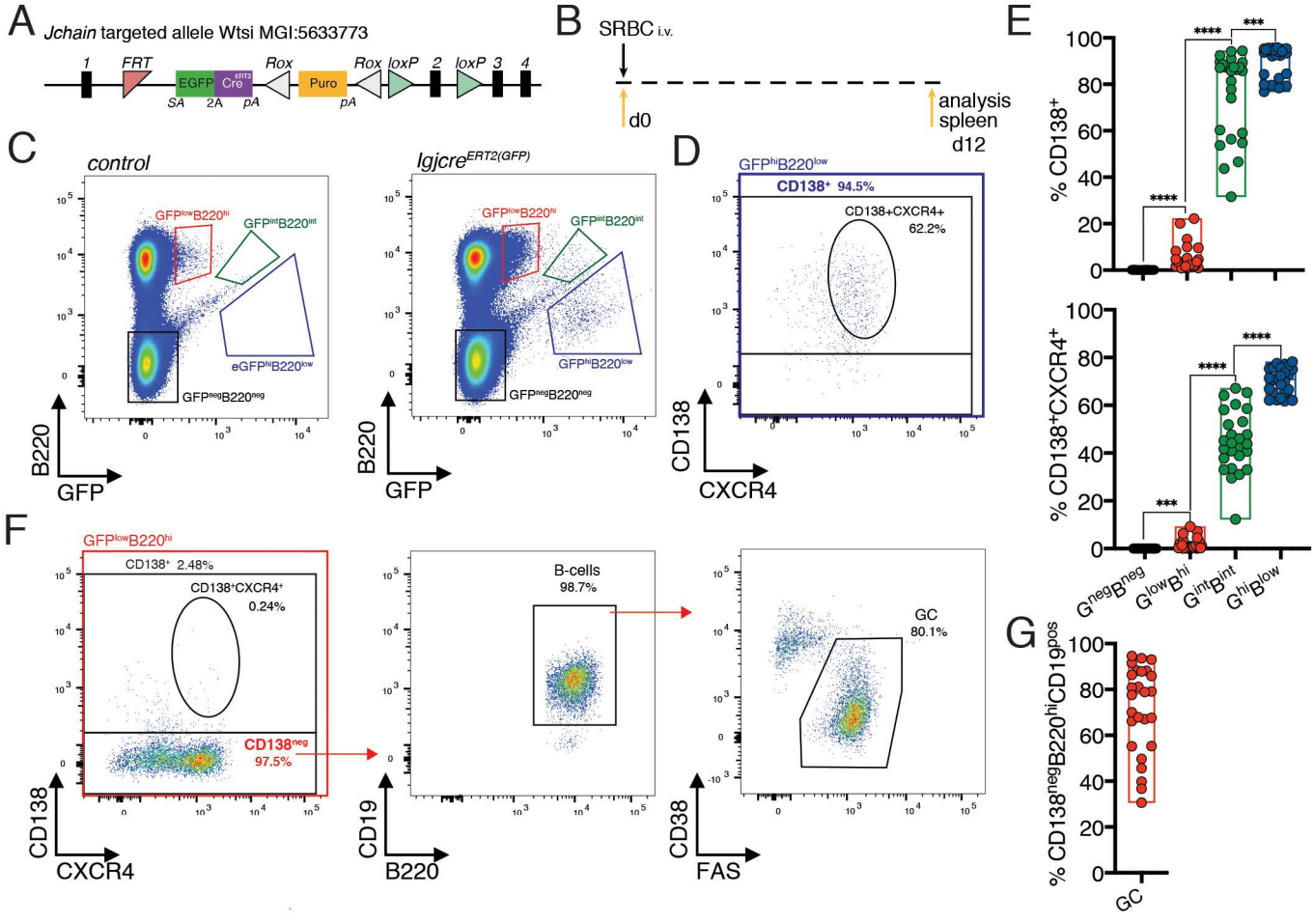

Xu A.Q. et al.

Figure 3:

Jchain expression correlates with IRF4 and BLIMP1 co-expression

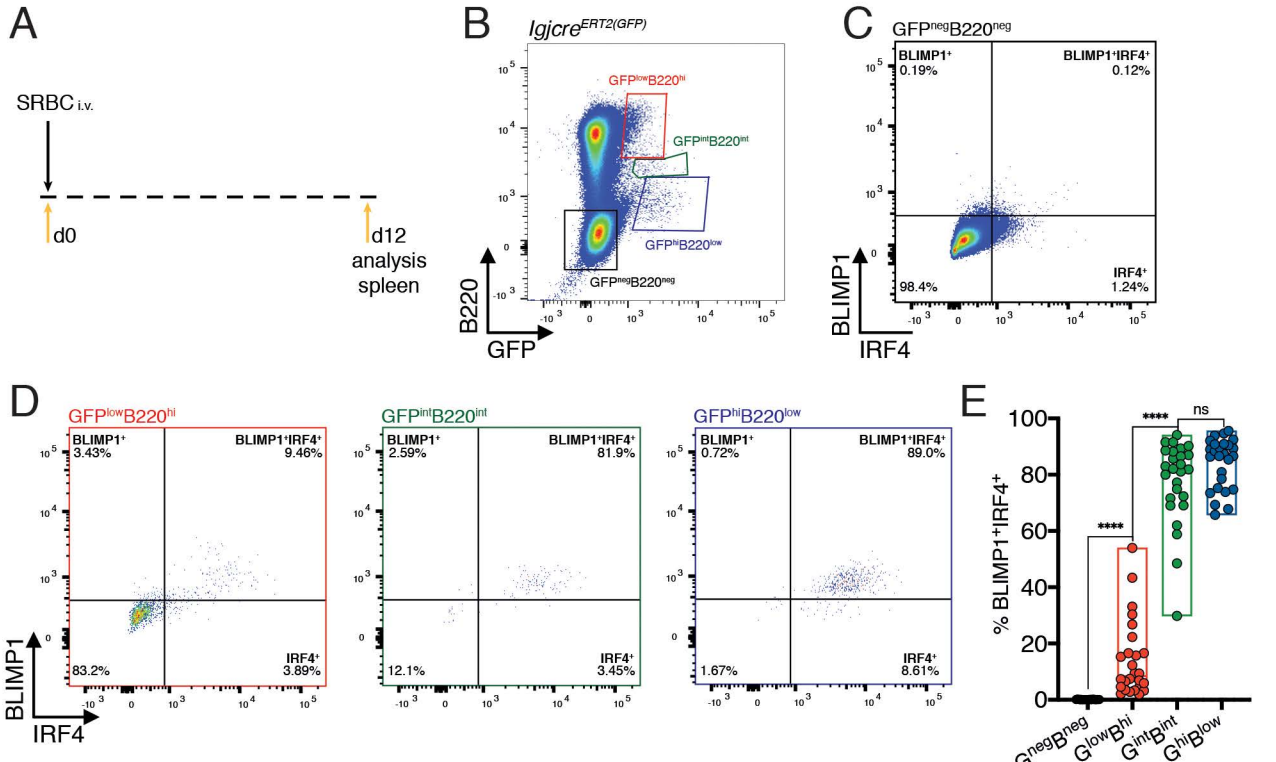

Xu A.Q. et al.

Figure 4.

Igjcre$^{ERT2(GFP)}$ mediated cre recombination is effective only in plasma cells

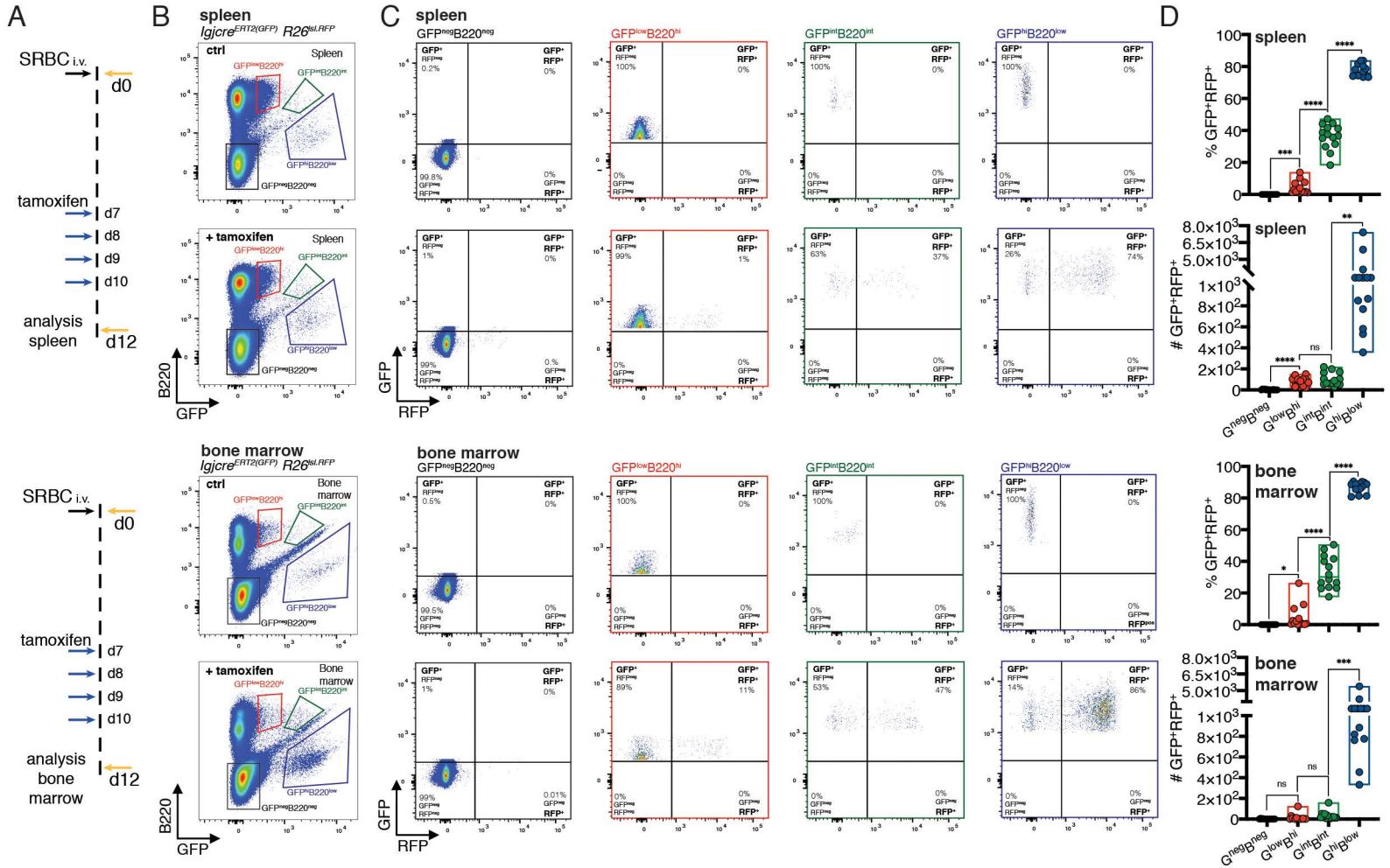

Xu A.Q. et al.

Figure 5.

Genetic manipulation using *Igjcre*$^{ERT2(GFP)}$ occurs across immunoglobulin isotypes

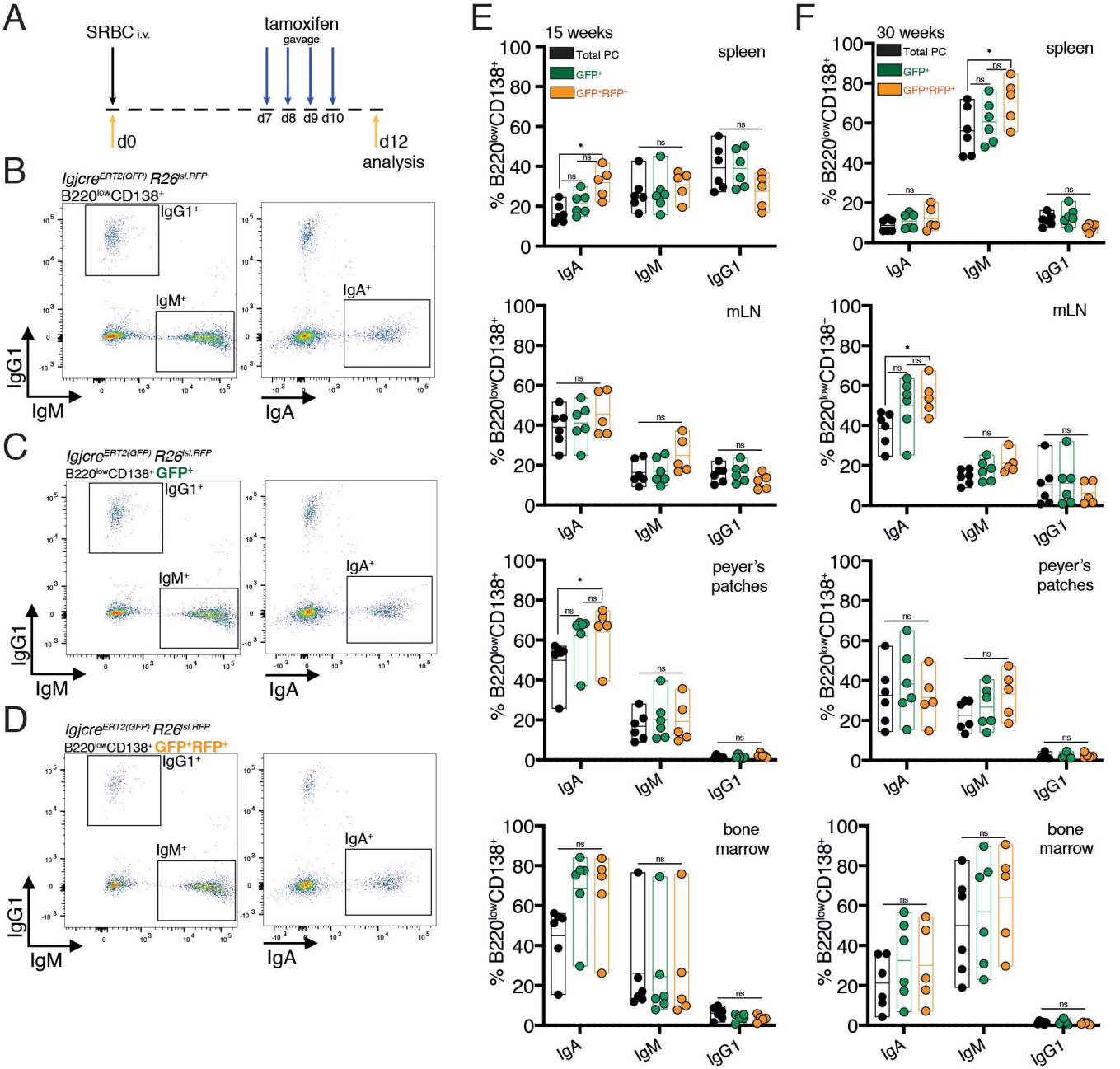

Xu A.Q. et al.

Figure 6.

Igjcre$^{ERT2(GFP)}$ allows lifespan studies and to trace long-lived plasma cells

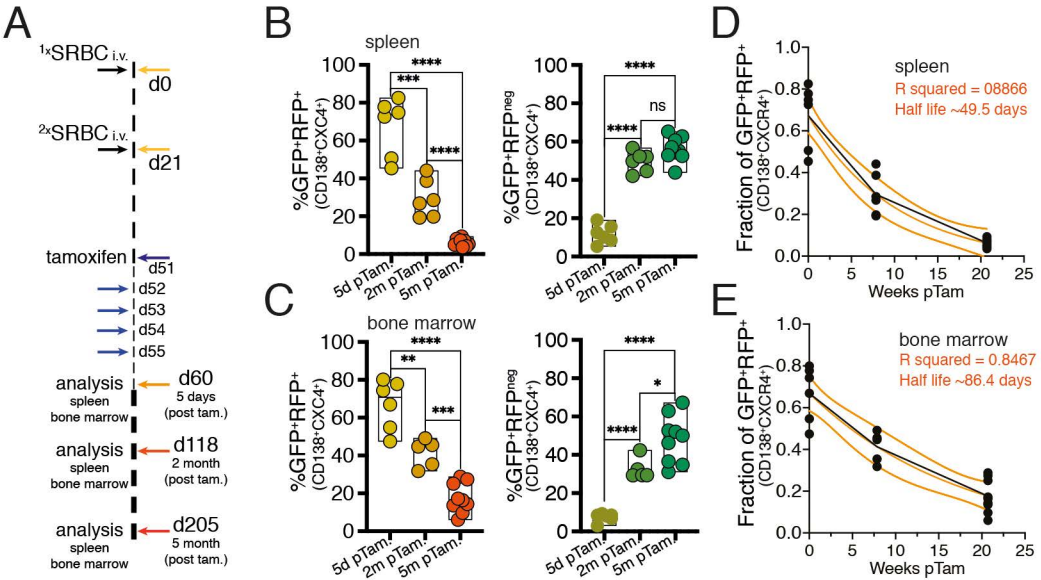

Xu A.Q. et al.

Figure S1.

Jchain expression in multiple stages of B cell development and other cell lineages

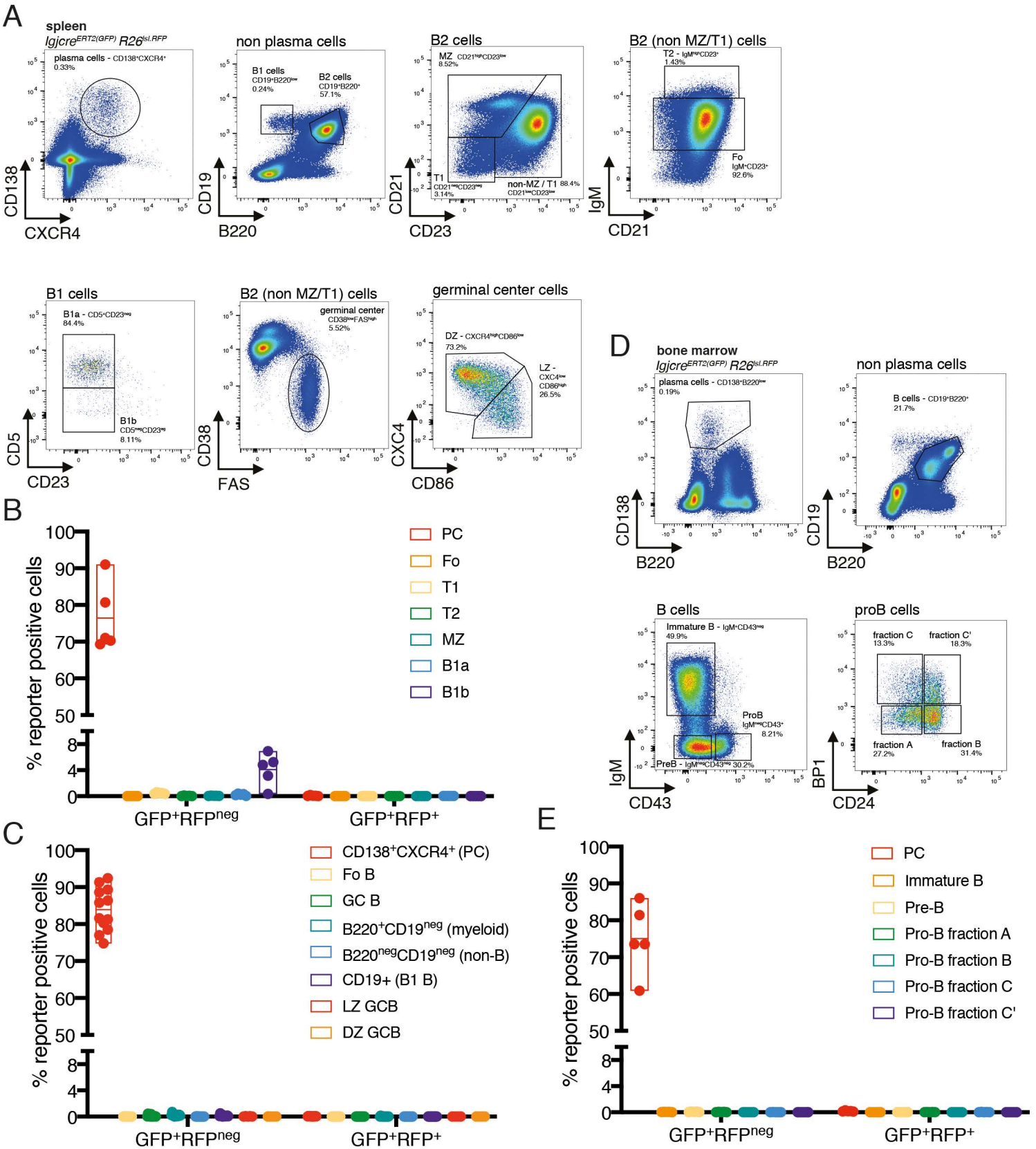

Xu A.Q. et al.

Figure S2.

Igjcre$^{ERT2(GFP)}$ mediated recombination *in vitro*

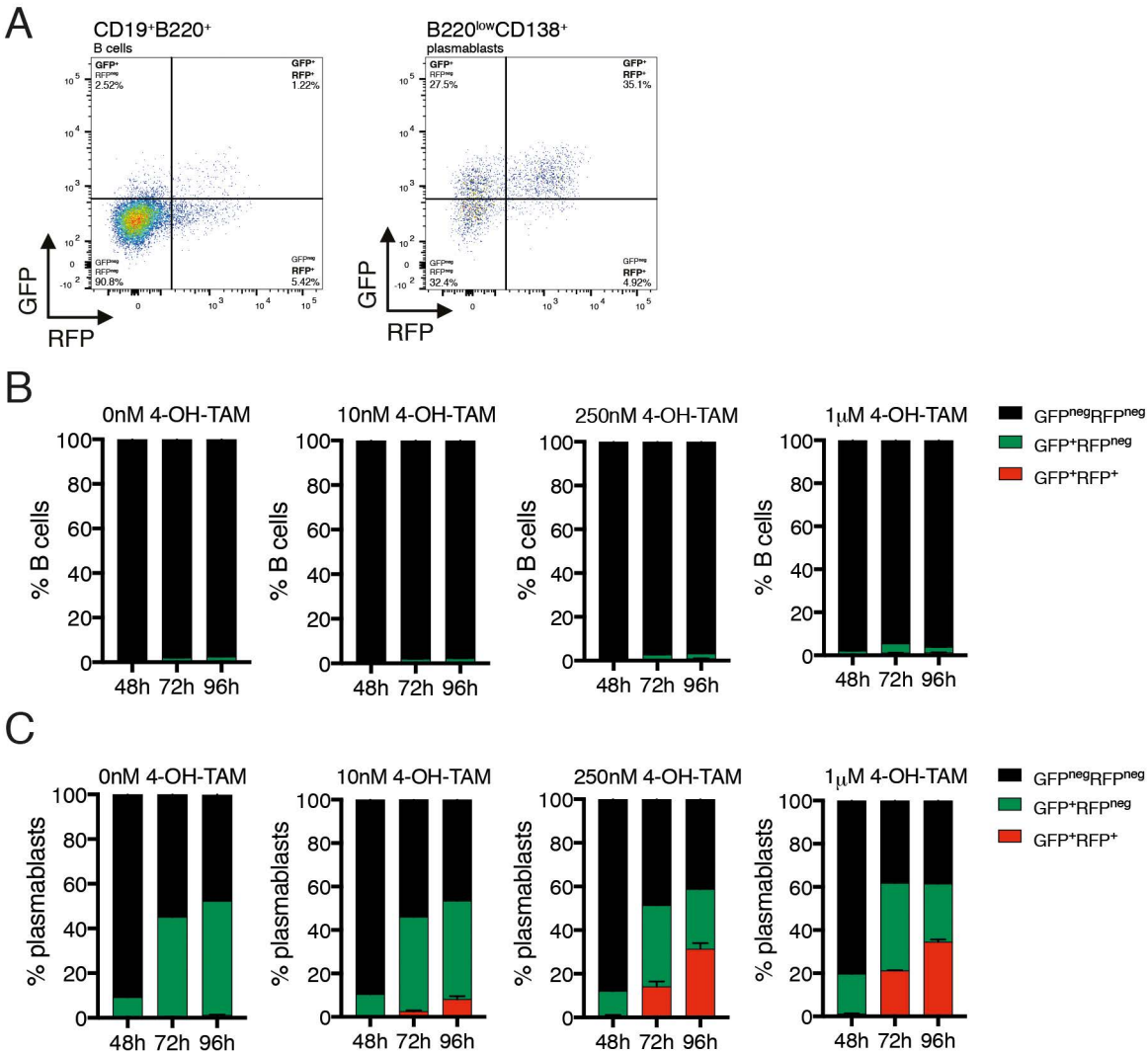

Xu A.Q. et al.